

The geometrical nature of optical resonances in nanoparticles

F. Papoff* and B. Hourahine*

*SUPA, Department of Physics, University of Strathclyde, 107 Rottenrow,
Glasgow G4 0NG, UK.(email: papoff@phys.strath.ac.uk, benjamin.hourahine@strath.ac.uk)*

We give a geometrical theory of resonances in Maxwell's equations that generalizes Mie formulae for spheres to any dielectric or metallic particle without sharp edges. We show that the electromagnetic response of a particle is given by a set of modes of internal and scattered fields and reveal a strong analogy between resonances in nanoparticles and excess noise in unstable macroscopic cavities. We give examples of two types of optical resonances: those in which a single pair of internal and scattered modes become strongly aligned in the sense defined in this paper, and those resulting from constructive interference of many pairs of weakly aligned modes, an effect relevant for sensing. We demonstrate that modes can be either bright or dark depending on the incident field and give examples of how the excitation can be optimized. Finally, we apply this theory to gold particles with shapes often used in experiments.

PACS numbers: 42.25.Fx, 78.67.-n, 42.25.Gy

The interaction of light with wavelength sized particles has been intensely investigated for more than a century, continuing to provide interesting and surprising results. This coupling is essential in single molecule spectroscopy and photon processes [1, 2], while interference between different scattering channels of particles produce classical analogues of quantum processes [3, 4], and carefully designed particles underpin the physical realization of metamaterials [5–7]. The basis all of these effects is the strong variation of particle-light interaction with wavelength. For particles much larger than the wavelength of light, resonances are described by closed orbits of light rays [8] inside the particle. This geometric approach becomes less and less effective as the size of the particle decreases, eventually requiring the solution of Maxwell's equations. Mie-type theories[9, 10], based on symmetry and coordinate separability, provide analytical description of resonances for a few specific shapes of particle. For spheres, a resonance occurs when the coefficient of one of the electric or magnetic multipoles in the field expansion becomes infinite for particular values of the particle radius, permittivity and susceptibility. In this framework, resonances are not connected to anything similar to energy levels (eigenvalues of the familiar hermitian operators of quantum mechanics), and do not show an obvious geometrical interpretation. Here we introduce an hermetian operator to reveal the geometrical nature of resonances in the Maxwell equations.

We consider metallic and dielectric particles without sharp edges and of dimensions of the order of the wavelength of the incident field or smaller, so that the interaction between light and matter inside the particle is described by local macroscopic permittivity and susceptibility. The tangential components of electric and magnetic fields E, H are continuous on passing through particle boundaries, and the energy scattered by a particle flows towards infinity. We use [11] six component vectors $F = [E, H]^T$ for electromagnetic fields; their pro-

jections, f , onto the surface of the particle are surface fields that form a space \mathcal{H} where scalar products are defined in terms of surface integrals. In this formalism the boundary conditions become

$$f^0 = f^i - f^s, \quad (1)$$

which has a simple geometrical meaning in \mathcal{H} : the projection f^0 of the incident field onto the surface is equal to the difference between the projections of the internal and scattered fields, f^i and f^s . This suggests that an external field with small tangent components can excite large internal and scattered surface fields provided that these cancel each other. This happens when the “angle” between these two fields, and therefore their difference, is small.

Importantly, for the particles considered here, sets of electric and magnetic multipoles that are linearly independent and complete in \mathcal{H} can always be found [12, 13]. Using these sets we then form separate orthonormal bases $\{i_n\}$ and $\{s_n\}$ for the projections of internal and scattered fields. These fields, which we call principal internal and scattering modes, are orthogonal to all but at most one function in the other space. For spherical particles, each pair of modes corresponds to a pair of electric or magnetic multipoles of Mie theory. For non-spherical particles, principal modes are instead combinations of different multipoles (although in some cases there can be dominant contributions from a specific multipole). We can find the internal and scattered fields for a particular incident field by decomposing this field into a sum of pairs of modes $f^0 = \sum_n a_n^i i_n - a_n^s s_n$, where $a^{i/s}$ are amplitudes of the internal and scattered principal modes for that specific incident field. The angle, ξ_n , between s_n and i_n is defined as

$$i_n \cdot s_n = \cos(\xi_n), \quad (2)$$

where we choose the arbitrary phase factors so that the scalar product is either positive or null. The terms on the

right-hand side of eq. (2) are the principal cosines introduced for the first time by Jordan in 1875 [14]. $\sin(\xi_n)$ is the orthogonal distance between s_n and i_n , and $\cos(\xi_n)$ their statistical correlation [15]. These angles are invariant under rotation and/or multiplication by a phase factor [16] and characterize the geometry of the subspaces of the internal and scattered solutions in \mathcal{H} . This geometry is induced by the particular particle through the surface integrals of the scalar products; its relevance to scattering and resonances has not been previously realized. The importance of the principal cosines is twofold: Theoretically they provide analytic equations for the coefficients of the internal and scattered principal modes, generalizing the Mie formulae and clarifying the nature of all scattering channels of a particle. Numerically, they allow us to reduce large matrices to their sub-blocks and eliminate the need of numerical inversion for the determination of the mode coefficients.

Minimization of $|f^0 - \sum_n a_n^s s_n + a_n^i i_n|$ leads to the equation

$$\begin{bmatrix} 1 & C \\ C^\dagger & 1 \end{bmatrix} \begin{bmatrix} \mathbf{a}^i \\ -\mathbf{a}^s \end{bmatrix} = \begin{bmatrix} \mathcal{I}^\dagger f^0 \\ \mathcal{S}^\dagger f^0 \end{bmatrix}, \quad (3)$$

where \mathcal{I}, \mathcal{S} are matrices whose columns are formed by the principal modes $\{i_n\}$ and $\{s_n\}$, respectively, 1 is the identity and $\mathbf{a}^i, \mathbf{a}^s$ are the coefficients of the principal modes in the field's expansion. The most important part of our theory is that principal modes are coupled pairwise, i.e. that the matrix C is diagonal. The interaction of particles with light can then be interpreted in terms of eigenvalues and orthogonal eigenvectors $w_n^\pm = (i_n \pm s_n)/\sqrt{2}$ of the hermitian operator in Eq.(3). However, away from the surface one measures either internal or scattered fields, so we transform the eigenfunctions, $\{w_n^\pm\}$, to find the coefficients of the principal modes:

$$a_n^i = \frac{i_n - \cos(\xi_n)s_n}{\sin^2(\xi_n)} \cdot f^0, \quad (4)$$

$$a_n^s = -\frac{s_n - \cos(\xi_n)i_n}{\sin^2(\xi_n)} \cdot f^0. \quad (5)$$

Here $i'_n = i_n - \cos(\xi_n)s_n$, $s'_n = s_n - \cos(\xi_n)i_n$ are bi-orthogonal to i_n, s_n ($i'_n \cdot s_n = s'_n \cdot i_n = 0$) with $i'_n \cdot i_n = s'_n \cdot s_n = \sin^2(\xi_n)$. a_n^i, a_n^s in Eqs. (4, 5) are found by projecting the incident field f^0 onto non-orthogonal vectors i_n, s_n and $\sin(\xi_n)$ is defined as the Peterman factor [17] that gives the order of magnitude of transient gain and excess noise in unstable cavity modes. Therefore the presence of strongly aligned vectors with $\sin(\xi_n) \ll 1$ is at the origin of large surface fields in nanoparticles as well as large transient gain and excess noise [18] in macroscopic unstable cavities and dissipative systems governed by non-hermitian operators [19]. However, the physical origin of the non-orthogonality of i_n, s_n is not dissipation, but the fact that internal and

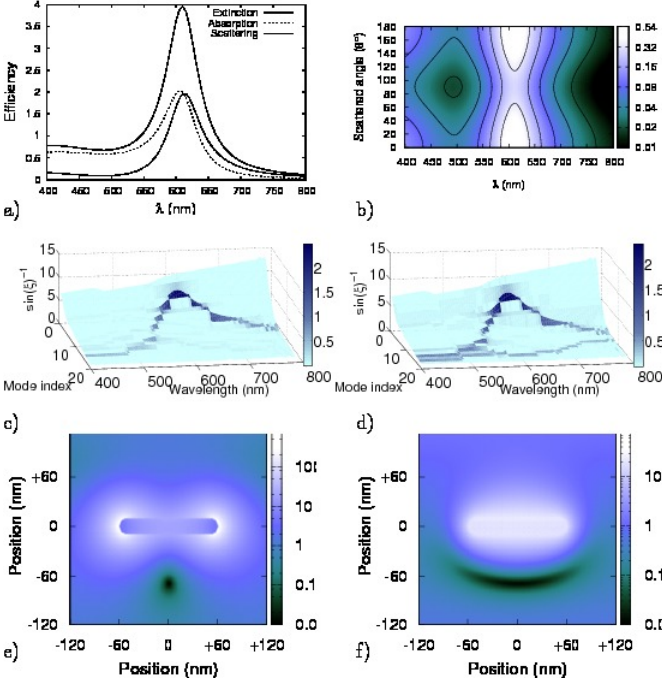
scattered fields are not modes of the hermitian operator and are correlated, even in the case of non-absorbing particles.

These surface modes and their amplitudes fully specify the electromagnetic behavior of the particle everywhere in space, for example electric currents within the particle and its surface plasmons can be found using the fields and the Ohm equation. Eqs. (4, 5) themselves have several important consequences. The left terms in the scalar products depend exclusively on the particle, this allows us to disentangle its properties from those due to the specific incident field. As an example, we now consider resonances. The principal modes and scalar products depend on the frequency dependent permittivity and susceptibility of the particle, and therefore the principal angles ξ_n change with the frequency of incident light. Internal and scattered coefficients diverge when the denominators of eqs. (4, 5) vanish. This happens when a pair of normalized internal and scattering modes are parallel. For a sphere the angular dependence of internal and scattered modes can be factored out and the condition $i_n = s_n$ can be recast in terms of the amplitude of the electric and magnetic components giving the Mie resonance condition. For physical particles, the linear independence and completeness of the principal modes makes perfect alignment impossible. So, as with spherical particles [20], actual resonances correspond to minimum angles ($\xi_n \neq 0$) of pairs in \mathcal{H} . One important difference from spherical particles exhibited by non-spherical structures is that the total flux of energy scattered or absorbed (integrals of the Poynting vectors over all directions) is given by the sum of principal mode contributions plus interference terms between modes, which are absent for spherical particles. Hence for non-spherical particles, strong peaks in the efficiencies can be caused by constructive interference within a group of modes. Furthermore, Eqs. (4, 5) show that modes can be “dark” for *specific* incident fields. The largest internal surface field is produced by an incident surface field parallel to i'_n : For well aligned modes, the coefficient $|a^i|, |a^s|$ are of the same order while, for weak resonances, $|a^s|$ is much smaller than $|a^i|$, leading qualitatively different absorption and differential scattering cross sections (DSCS). Similar effects happen for an incident surface field parallel to s'_n , exchanging $|a^i|$ and $|a^s|$.

Regarding numerical calculations, we remark that $\sum_{n=1}^N a_n^i i_n, \sum_{n=1}^N a_n^s s_n$ converge to the exact fields for $N \rightarrow \infty$ at any point inside and outside the particle [11, 21], and $|f^0 + \sum_{n=1}^N a_n^s s_n - a_n^i i_n|$ allows us to verify the accuracy of the calculations for finite N [13]. Most importantly, the form of Eqs.(4,5) remains unchanged as $N \rightarrow \infty$, even if θ_n, i_n, s_n change [16].

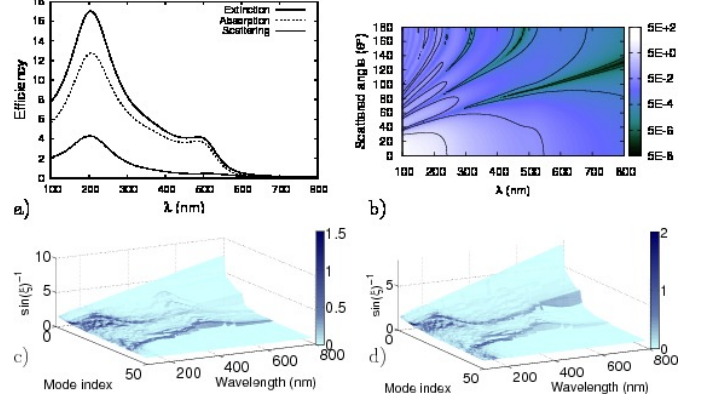
We now consider light interaction with some specific gold particles, using a fitted dielectric function [22]. Fig. 1 shows calculated near and far field properties of a rounded nanodisc (height 20 nm and diameter 120 nm),

FIG. 1: (Color online) Calculated modes of the gold nanodisc. a) Scattering, absorption and extinction efficiencies, showing the strong resonance at 613 nm. b) The DSCS as a function of wavelength, illustrating the dipole nature of this particular resonance. c) and d) Excitation paths of scattered and internal fields over the principal angle landscape. e) and f) Near field plots of the dipole resonance disc viewed parallel and perpendicular to the electric field of the axial light.



illuminated axially by plane-wave light. We find a strong dipole resonance (fig. 1a,b) at 613 nm, in agreement with a previous experimental and numerical investigation [23]. Figs. 1c,d) show the landscape of principal mode angles, which are intrinsic properties of the particle, as a function of mode index and wavelength of incident light. The “height” of this landscape is $\sin(\xi)^{-1}$, the largest value of eq. 4 and eq. 5 for $|f^0| = 1$, while the amplitudes of the internal and scattered principal modes due to the *specific* axial incident field are shown overlaid on top. These *excitation paths* demonstrate that the observed resonance is a Mie-like single principal cosine pair, which comes into maximum alignment (its smallest value of ξ) at the resonance. Other strongly aligned dark modes are also present, but not excited by this particular incident field. The internal field also contains a second more weakly aligned excited mode, where its counterpart in the scattering field is not excited. This mode and of the resonant mode have quasi-degenerate principal angles on the shorter wavelength side of its peak; this strengthens the internal field and explains the appreciable asymmetry of the absorption efficiency. The near field around the particle at resonance (fig. 1e,f) shows that the resonance is an

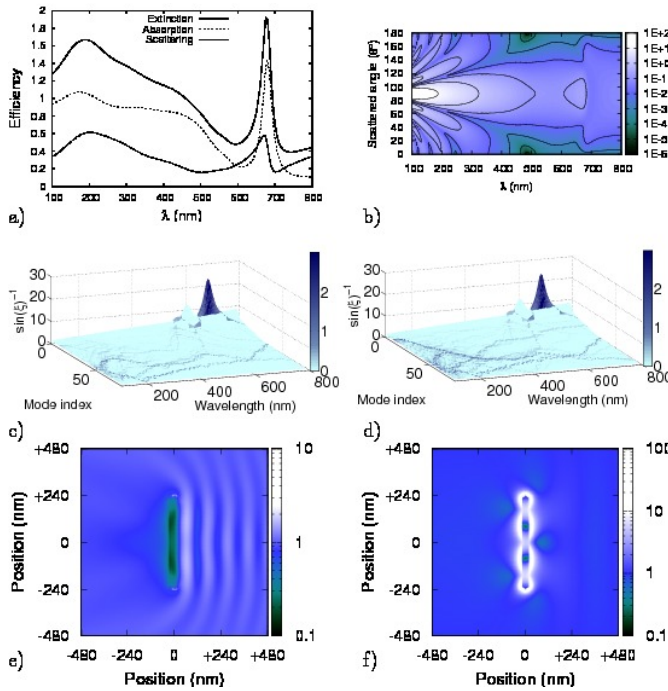
FIG. 2: (Color online) Calculated optical modes of the rounded nanorod when illuminated axially. a) Scattering, absorption and extinction efficiencies showing the 205 nm mode and weaker absorption peak at 486 nm. b) DSCS showing the strong forward scattering of light by the particle. c) and d) Scattered and internal excitation paths, showing the composite nature of the modes.



electric dipole. For non axial incidence, the main peak is smaller due to a weaker coupling with the resonant mode.

Fig. 2a,b) shows the calculated optical efficiencies and DSCS of a 480 nm long rod with diameter 40 nm, illuminated axially by plane-wave light. There is a strong resonance at 205 nm and a weaker absorption peak at 486 nm (an extremely weak corresponding scattering feature is present at ~ 515 nm). The DSCS demonstrates that this particle strongly scatters this incident light forward, particularly at short wavelengths. The peak at 205 nm is not a single mode, but instead the excitation amplitudes of the principal modes (fig 2c,d) show it to be due to constructive interference of contributions from a group of several weakly aligned principal mode pairs. Collectively these modes very efficiently extract energy from the incident field. Such multimode resonances are potentially useful for sensing applications because interference between different scattering channels leads to enhanced sensitivity to perturbations near to the scattering surfaces. The absorption feature at 486 nm is also due to a group of mode pairs, in which only the internal modes are excited, all becoming more strongly aligned at around this resonance. Fig. 3 shows the same particle illuminated equatorially with an incident light polarization of 45° with respect to its long axis. Analyzing other particles with the same diameter but varying length, we find that the broad feature at around 200–450 nm, containing structures similar to the composite modes of Fig. 2, is insensitive to the particle length. It also shows no clear hot or cold spots (see fig 3e). The sharp resonance at 676 nm shifts with the length of the rod and its surface field has the strong nodal local structure (Fig. 3f)

FIG. 3: (Color online) The particle from fig. 2, but illuminated from the side with an incident light polarization of 45° with respect to its long axis. a) Far field scattering efficiencies showing the presence of both a broad feature similar to Fig. 2 at around 200–450 nm and also a sharp resonance at 676 nm. b) The DSCS for equatorial illumination c) and d) Scattered and internal excitation paths; the principal angle landscape includes additional modes that cannot be excited by symmetry for axial incidence (cf. Fig. 2). The sharp mode is again a single well aligned principal pair, the best aligned of three (and the only one excited by this field). e) and f) Near field for the 480 nm rod, shown at the broad feature (207 nm) and at the “waveguide” Mie-like mode at 676 nm.



of a “waveguide” mode on the long axis. The excitation paths (Fig. 3c,d) are shown including additional modes that cannot be excited by symmetry for axial incidence (cf. Fig. 2). As with the disc, the sharp resonance is again a single well aligned principal pair, the best aligned (and the only one excited by this field) of three such waveguide modes that shift with the length of the particle.

In summary, we provide a geometrical explanation for resonances that generalizes Mie formulas for spheres to all isotropic particles without sharp edges and reveal strong analogies between resonances in nanoparticles and excess noise in macroscopic cavities. We show that there are sharp resonances caused by strong alignment between one internal and one scattered modes and broad resonances due to several pairs of internal and scattered modes with weak, but similar, alignment. Our equations indicate that any observation depends both on the structure of the principal modes, which are an intrinsic

property of the particle, and the way an incident field couples to these modes. In particular, there can be resonant modes that are essentially dark with respect to a given incident field. The amplitudes of the principal modes specify the field both inside and outside the particle. This geometric approach is applicable to a large class of processes, where the interaction between the system and the environment is described by a set of functions complete at the boundary of the system, including other scattering processes such as of acoustic or electron waves, and coupling to optical cavities.

- [1] D. Graham and R. Goodacre, *Chem. Soc. Rev.* **37**, 883 (2008).
- [2] T. Aoki, B. Dayan, E. Wilcut, W. P. Bowen, A. S. Parkins, T. J. Kippenberg, K. J. Vahala, and H. J. Kimble, *Nature* **443**, 671 (2006).
- [3] B. Lukyanchuk, N. Zheludev, S. Maier, N. Halas, P. Nordlander, H. Giessen, and C. tow Chong, *Nature Mater.* **9**, 707 (2010).
- [4] N. Liu, L. Langguth, T. Weiss, J. Kstel, M. Fleischhauer, T. Pfau, and H. Giessen, *Nature Mater.* **8**, 758 (2009).
- [5] J. Schuller, E. Barnard, W. Cai, Y. C. Jun, J. White, and M. Brongersma, *Nature Mater.* **9**, 193 (2010).
- [6] Q. Zhao, J. Zhou, F. Zhang, and D. Lippens, *Materials Today* **12**, 60 (2009).
- [7] J. Pendry, D. Schuring, and D. Smith, *Science* **312**, 1780 (2006).
- [8] G. Roll and G. Schweiger, *J. Opt. Soc. Am. A* **17**, 1301 (2000).
- [9] G. Mie, Leipzig, *Ann. Phys.* **330**, 377 (1908).
- [10] Y. Han and Z. Wu, *Applied Optics* **40**, 2501 (2001).
- [11] K. Holms, B. Hourahine, and F. Papoff, *J. Opt. A: Pure Appl. Opt.* **11**, 054009 (2009).
- [12] A. Aydin and A. Hizal, *Journ. Math. Anal. and Appl.* **117**, 428 (1986).
- [13] A. Doicu, T. Wriedt, and Y. Eremin, *Light Scattering by Systems of Particles* (Springer, 2006).
- [14] C. Jordan, *Buletin de la Société Mathématique de France* **3**, 103 (1875).
- [15] E. Hannan, *J. Aust. Math. Soc.* **2**, 229 (1961/1962).
- [16] A. Knyazev, A. Jujushvili, and M. Argentati, *Journ. of Func. Analys.* **259**, 1323 (2010).
- [17] G. New, *Journ. Mod. Optics* **42**, 799 (1995).
- [18] W. J. Firth and A. Yao, *Phys. Rev. Lett.* **95**, 073903 (2005).
- [19] F. Papoff, G. D’Alessandro, and G.-L. Oppo, *Phys. Rev. Lett.* **100**, 123905 (2008).
- [20] M. I. Tribelsky and B. S. Lukyanchuk, *Phys Rev. Lett.* **97**, 263902 (2006).
- [21] T. Rother, M. Kahnert, A. Doicu, and J. Wauer, *Prog. Electromag. Res.* **38**, 47 (2003).
- [22] P. G. Etchegoin, E. C. Le Ru, and M. Meyer, *J. Chem. Phys.* **125**, 164705 (2007).
- [23] J. Aizpurua, P. Hanarp, D. Sutherland, M. Kall, G. Bryant, and F. J. G. de Abajo, *Phys. Rev. Lett.* **90**, 057401 (2003).